In-Silico Evaluation and Development of a Nanoemulsion System of *Withania somnifera* Phytoconstituents for Multi-target Intervention in Alzheimer's Disease

Snigdha Singh[1] *Divya Jindal*[1] *Mohd Maksuf Ul* Haque[1], *Malika Kapoor*[1,2], *Manisha Singh*[1,3,4*]

[1]*Department of Biotechnology, Jaypee Institute of Information Technology, Noida, U.P., India*
[2]*Indian Institute of Technology Bombay Monash Research Academy, Mumbai, India*
[3]*Faculty of Health, Graduate School of Health, University of Technology Sydney, Australia*
[4]*Woolcock Institute of Medical Research, University of Sydney, Sydney, Australia*
*Corresponding author: manisha.singh@mail.jiit.ac.*in

Abstract: Neurodegenerative diseases, especially AD, is becoming a worldwide health burden with characteristic features such as neuronal loss, synaptic impairments, progressive degeneration of neocortex and aggregation of amyloid (β). Current drugs used to treat Neurodegenerative diseases merely offer symptom relief and do not alter disease course owing to poor BB barrier (BBB) permeability and poor pharmacokinetics. Nanotherapeutics are thus being investigated as potential tools to improve specific delivery of compounds to the brain. In this study the neuroprotective efficacy of *Withania somnifera* extract-loaded nano-emulsion systems has been demonstrated through interaction of several molecular targets involved in AD. The in silico molecular docking studies clearly established significant binding energy of the investigated bioactives
(withanolides, withaferin A, quercetin, L, ascorbic acid etc,) towards major therapeutic targets involving AD (AChE, BChE, NMDA receptor, BACE1, MAO, A, ApoE) and so indicate their significant activity against multi targets of AD. Different oils, surfactants and co, surfactants were chosen and studied for extract solubilization for nano-emulsion formation. Almond oil, triacetin and ethanol were selected based on solubilization for formulation development adopting water titration method. A water titration employing Smix (surfactant and co, surfactant) of 2:1 ratio led to the formation of stable oil, in, water nano, emulsion system. The developed formulations showed physicochemical parameters within acceptable limits: PH (3.74, 4.20), conductivity (61.3, 86.8 m S/m), viscosity (34.3, 41.1 c P) and density (0.964 g/m L). Dynamic light scattering particle size analyser revealed average particle sizes from 185.5 to 212 nm, with value of zeta potential between 28 and 33 mV. Spherical structures within the nanometric range were confirmed using transmission electron microscopy, and extract encapsulation was detected using FTIR. In general, the nanoemulsion loaded with produced here showed adequate physicochemical stability and ability to target multiple pathologies. Further, we need to do pharmacokinetic and pharmacodynamic studies in order to determine therapeutic effects in the brain.

1. Introduction

As the world's life expectancy continues to climb and the aging ratio sharpens, the health consequences of neurodegenerative disorders (NDDs) are getting worse. Over 50 million individuals worldwide suffer with dementia, and the annual cost of medical care exceeds 800 billion US dollars [2]. One of the most prevalent and rapidly progressing types of neurodegenerative disorders is Alzheimer's disease (AD) [1]. AD is a chronic, irreversible CNS disorder associated with progressive cognitive impairment, memory deficit and visuospatial dysfunction complemented by behavioural symptoms and psychiatric features [3]. According to estimates, AD will impact roughly 65.7 million people in 2030 and 115 million by 2050, making it a significant global public health concern [4]. It is exponentially more common after the ages of 60-65 [5,6]. The CNS which include the brain and spinal cord, controls sensory perception, motor coordination, cognition and internal physiological process. Neurons (the basic functional unit of the nervous system) are composed of a cell body, dendrites for signal reception, and axons for signal propagation [4].

However, unlike most other cell types, neurons have a limited regenerative capacity which contributes to the complexity and poor prognosis of NDDs [5]. Such disorders include Alzheimer's disease (AD), Parkinson's disease (PD), Huntington's disease (HD), Amyotrophic lateral sclerosis (ALS) and Multiple sclerosis (MS) [6]. The pathophysiology of Alzheimer's Disease is multifaceted with several overlapping hypothesis [6]. The cholinergic hypothesis (another direction in the degenerative pathway) states that the cognitive deficits associated with AD are determined by reduced levels of acetylcholine (AChE) in the synapse caused by increased AChE activity [7]. Butyrylcholinesterase (BuChE) has also been linked to the deposition of amyloid plaques, prescribing dual AChE administration. The amyloid cascade hypothesis explains the excessive synthesis and accumulation of, amyloid (β) [8]. peptides in senile plaques resulting in extracellular plaque formation and neuronal toxicity. Oxidative stress is proposed as a further causative pathology, with excessive free, radical (ROS) production and mitochondrial damage being the cause of the neuronal cell death, often via a MAO, catalysed process [9]. Finally, increased excitation at the, amino, 3, hydroxy, 5, methyl, 4, isoxazole propionic acid (AMPA) receptor caused by excess glutamate results in high calcium levels leading to apoptosis. [9-10] As such, the most widely used therapies for treating AD only provide symptomatic relief and have no impact on the progression of the disease [11] Attention has been focused

recently on NPs and phyto therapeutics in the management of AD. Traditional Ayurveda, practiced for thousands of years, has identified many plant, derived compounds with pleiotropic pharmacological actions. Phytochemicals can modulate AChE, BuChE, MAO, NMDA receptor and, secretase (BACE, 1) whilst exhibiting antioxidant and anti - inflammatory properties [11] The neuroprotective potential of medicinal plant such as *W. somnifera* (WS) has been demonstrated in preclinical models. Numerous plants with medicinal value are known to be crucial in treating central nervous system (CNS) disorders. Amidst all such plants WS, the ancient tree is extensively explored for innumerable treatment strategies against various diseases in Indian traditional medicinal therapy. Extracts of WS made from the leaves of the tree were chosen for the present study.

However, BBB permeation is the major obstacle for CNS drug delivery, as it prevents most pharmacologically active compounds from reaching their receptors in the brain. [12]. Novel strategies employing effective drug delivery systems can help to overcome this restriction and deliver more drugs into brain tissue, with favourable pharmacokinetic characteristics and negligible systemic toxicity [12-13]. The delivery systems which are gaining increased interest for this purpose are Nano, based delivery systems. Nanoemulsions (NEs) owing to their small droplet sizes, large interfacial areas, and lipophilicity can enhance solubilization of drugs, stability and permeation across BBB. They provide controlled drug release, increase bioavailability, decrease toxicity and prolong residence time, when combined with mucoadhesive polymers [14] This delivery system has shown promising capabilities in enhancing phytocompounds delivery to the CNS. In summary, AD represents a major worldwide health burden with a dearth of available therapies. Natural phytocompounds can provide multitarget neuroprotection albeit this approach has yet to see success during pharmacokinetic and delivery considerations. Combining phytotherapeutic with novel multi, functional NEs based drug delivery systems is a rational strategy to potentially boost various BBB delivery considerations and achieve a wider therapeutic window.

2. Materials and Methodology

2.1 *In -Silico* Analysis of Phytocompounds of WS

Molecular docking was performed for WS ligands against AD targets: AChE (4EY6), BuChE (10PM), NMDA (1PBQ), MAO-A (2Z5X), and BACE1 (4X7I). Ligands were sourced from PubChem, Table 2.1 shows the various classes of phytochemicals that are present in WS, and target protein PDB files were retrieved from RSCB PDB. Proteins were prepared using Schrödinger, involving H-atom addition, bond order optimization, filling missing residues, disulfide bond formation, and water removal (>5.00 Å from het groups). Heteroatom protonation states were generated using Epik at pH 7.0 ± 2.0, and chain A of the protein was selected for further analysis. The proteins were subsequently optimized using PROPKA at pH 7.0, and acetylcholinesterase (AChE) was minimized to an RMSD of 0.30 Å using the OPLS_2005 force field[25,26]. The active site was defined by the co-crystallized ligand location. Ligands were prepared using Ligprep (OPLS_2005), with ionization states generated by Epik and Ionizer (pH 7.00 ± 2.00) [28,29]. Unwanted ions and water were removed using Desalt. Receptor Grids were generated using the Glide Tab, centred on the co-crystallized ligand binding site to ensure site-specific docking, with grid size adjusted to the active site dimensions. Binding affinities (free energy of binding) were calculated using GLIDE

Table 2.1 The various classes of phytochemicals that are present in *WS*

Class	Phytochemicals (Ligands)
Alkaloids	Hygrine, Trigonelline, Anahygrine, Cuscohygrine, Withasomnine, Somnifericin, (-)-Anaferine, Tropine, Somniferine
Steroids & Steroid Lactones	Guggulsterone, Ergosterol, Viscosalactone B, Withanolide A, Withanolide B, Withanolide E, Withanolide F, Withanolide J, Withanolide M, Withanolide N, Withanolide O, Withanolide P, Withanolide S, Withanone, Withanoside X, Withanoside XI, WithanosideVIII, Hydrocortisone sodium succinate, Withaferin A, Withanolide Q, Withanolide R, Coagulin Q, Sitoindoside IX, Hydrocortisone, Phytosterols, Daucosterol, Delta-7-Avenasterol

Table 2.1 The various classes of phytochemicals that are present in *WS*

Carboxylic Acids & Derivatives	N-(2-Cyanoethylene)urea, Trans-4-Hydroxy-L-proline, DL-Valine, L-cysteine, L-proline, DL-Tryptophan
Terpenoids (Non-Steroidal)	beta-Amyrin, beta-boswellic acid, Ginsenosides, Oleanolic acid
Other Heterocyclic Compounds	Nitrazepam, 1,4-Dioxane, Quercetin, Scopoletin
Miscellaneous	Octacosane, Hydroxyacetone, Mycothione, Resveratrol

The Extra Precision (XP) tool of the Glide software in the Schrodinger suite was used for ligand docking. The pregenerated glide grid file was used to attach the produced protein and ligand. The OPLS-AA non-bonded ligand-protein interaction energy was calculated using Glide's produced and reduced poses. Ligand-protein interactions, including interaction types and involved amino acids, were visualized using a ligand interaction diagram. Binding affinities and observed interactions were compared to assess potential ligands for Acetylcholinesterase [30].
Free energies of the complex were calculated using the Prime MM GBSA panel, providing the MMGBSA_dG_Bind value [31].

2.2 Preparation of WS Extract

Purified extract of WS is procured from Vital Herbs Company, Delhi. The extract of plant was further prepared using Soxhlet extraction with water, ethanol, and ethanol/water (50:50) as solvents. The ethanol was evaporated using a rotary evaporator after the Soxhlet extraction, and the water was removed using an incubator on 37°C. The dry end-products were kept at 20°C in glass containers, away from light [38]

2.3 Quantitative estimation

Various secondary metabolites from plant are known for their aromatic and potential medicinal properties. Thus, quantification of these metabolites was observed with significant phytochemicals present as phenolics and flavonoid. WS extract sample was prepared by mixing 50 mg/ml solution of WS in 5% ethanol (500µl), and then made up to the volume of 1 ml with aqueous phase.

2.4 Chromatographic analysis of WS

Ions from the test samples are separated out based on their mass to charge ratio (m/z) during the ionization process by applying an electric or magnetic force field. The test samples are exposed to vacuum binary pump system where they get vaporized into ionized molecules by ESI (electro spray ionization) and thereafter, in the mass analyzer unit molecules are segregated on the basis of their m/z ratio they possess. The detector unit records the ion flux passing through it, as an electric current in the form of mass spectrum [39]. The isocratic mobile phase was made with ethanol (80%) and Phosphoric acid (0.3%) in the ratio of 1:1, filtered through a 0.45 µm filter embedded filter unit and ultrasonicated for 15 minutes before use [40]. Also, the buffer preparation for test sample was done with 40mM SDS, 25mM phosphoric acid (pH 2.8) and was detected at 190 nm with separation voltage of -17.5 kV to -20 kV. Standard graphs were plotted for Quercetin, Nitrazepam and L-ascorbic acid compounds with their respective stock solutions (100ng/ml). The standard solutions were prepared in MeOH (80%) and filtered through 0.45µm nylon syringe filter. The prepared solutions of Quercetin and Nitrazepam were injected (10µ L) in to the pump system. The run time and the peak areas representing compound concentration for each of the standard compounds were recorded. Thereafter, the extract solution of 1 mg/ml was prepared in 80% MeOH and filtered through syringe filter (0.45µm membrane). Then it was directly infused into the electron spray interface (at positive ion mode for identifying and quantifying selected phytocompounds [41]

2.5 Preparation of WS Extract-Loaded Nanoemulsions

The solubility of extracts in different excipients (Oils - isopropyl myristate (IPM), Almond oil, Jojoba oil, Olive oil, Castor oil, Linseed oil, Tea tree oil; Surfactants – TPP, Triacetin (glycerol triacetate, PEG, Pluronic acid, PVP, PVA, Tween 20, Tween 80; Co - surfactants - Ethanol, Isopropanol) was determined by combining an excess amount of extract (5 mg) in 1 ml of each screened excipients (oils, surfactants, and co surfactants) everyday, separately in glass vials and keeping them in shaking incubator on room temperature at 200 rpm for overnight. After 24hours 5 mg of extract is added, when the extract has completely dissolved in the excipients [44]. Finally, they were

analysed by spectrophotometric method for quantification of flavonoid and phenolic compounds. The excipients that showed highest *WS* solubility were short listed for further formulation process.

To prepare the successful NE formulation from the selected excipients (oil, surfactant and co surfactant), water titration method was opted and titration of various excipients combination ratios were tried followed by their evaluation of stability and transparency [44]. First, several S_{mix} ratios of surfactant (1:0, 1:1, 2:1, 3:1, 4:1, 5:1 and 6:1) were added to the oil phase to prepare the NE system. After being well combined and vortexed, this mixture was titrated with an aqueous phase. Every excipient listed above was added while being constantly agitated, and were selected based on visual examination for any phase separation, breaking, precipitation, transparency, and foaming effects.
[45].

2.6 Preparation of Pseudo-Ternary Diagram

Pseudo ternary diagram representing different zones of different types of nanoemulsions. Excipients (oil, surfactants, and co-surfactants) that demonstrated maximal solubility were used to create pseudo-ternary phase diagrams using Origin Pro 2021 software based on the findings of the solubility analysis tests. In the experiment, the surfactants and co-surfactants were taken in various ratios and referred to as S_{mix}. Additionally, 16 distinct combinations of Oil and S_{mix} were taken for the investigation, ranging from 1:9 to 1:2 (9 combinations), 3:7, 4:6, 5:5, 6:4, 7:3, 8:2, and 9:1. **2.7 Characterization of Optimized Formulations**

a) Thermodynamic Stability Studies

The optimized formulations which were selected after plotting the pseudo ternary phase diagrams were selected to store at 4°C for 3 days followed by 45°C again for 3 days and this cycle was again repeated for 6 times. These samples were periodically checked for any kind of turbidity, clarity or aqueous phase loss [46]. To evaluate the stability of nano-emulsions during freezing and thawing, for the next three days the formulation was stored at -20 °C and then at 25°C for next three days. This process was repeated 6 times and checked regularly for any kind of creaming, frothing or phase separation phenomenon [46]. The test samples batches, which cleared the above stated tests (A, B) were subjected to speed stress test. The samples were centrifuged at 11200 Xg for 30 minutes and were checked for their physical stability. Then those formulations which didn't showed any phase inversion, aggregations, creaming and cracking were short listed. Lastly, the sample batches which cleared the above-mentioned tests (A, B, and C), were then dispersed in excess of water to check their dispersibility and non-coagulative properties. Formulations (WSNE) which passed all the above-mentioned tests of thermodynamic stability testing were further subjected for the next level of characterization.

b) Particle Size Analysis (PSA) And Polydispersibility Index (PDI)

For analyzing the particle size, dynamic light scattering (DLS) method was used which calculated the average particle size on the basis of dynamic fluctuation of scattered light intensity [47]. The mentioned process depends on the Brownian motion that illuminates the particles with a laser and examines the intensity disparity in the light scattering [48]. The test samples (WSNE) were sonicated for 30minutes. The prepared samples were then loaded in the PSA cuvette, to analyze the average PSA and PDI **c) Zeta Potential (ZP) Analysis**

Zeta potential is a magnitude index of repulsive electrostatic interaction among the particles caused by the charge present on the particle surface diffused in the solution hence, depicting the dispersion stability. The ZP of the WSNE droplets exhibits the electric charge among the shear plane of the outermost external layer and the total quantity of solution. This interaction is effectively used to confirm the property of dispersions. The WSNE formulation was sonicated for 30minutes and then loaded in the zeta sizer cuvette, to analyze the ZP. **d) Transmission Electron Microscopy (TEM)**

The optimised WSNE sample was diluted 100 times in distilled water and sonicated for 30 minutes. The samples were fixed by adding phosphotungstic acid(0.02 mg/ml) on carbon-coated copper grids, and blotted after 30 seconds, the image scans of selected regions were recorded at specific magnifications.

e) Measurement of Physicochemical Parameters

pH of the optimised formulation of WSNE was measured with the calibrated digital pH meter (Mettler Toledo MP 220, Greifensee, Switzerland). The viscosity of nano-emulsions is a measurement of the internal flow resistance and a sign of the fluid's consistency. To measure the viscosity of the optimized sample, 5 ml WSNE was taken and through viscometer the viscosity index is measured. Since, the aqueous phase is present in NE, the conductivity measurement reflects the continuous phase and tends to either increase or remain almost equivalent to water. A 5 ml colloidal solution of WSNE was tested on a conductometer (CM 180, Elico, India) at a steady frequency of 1 Hz.

3 Results and discussion

3.1 Docking Energy Calculation using Glide

Molecular docking was performed using the Glide program (Schrödinger) to investigate the binding affinities of WS against selected neurodegenerative disease targets: Monoamine oxidase A (2Z5X), NMDA (1PBQ), Butyrylcholinesterase (1OPM), Acetylcholinesterase (4EY6), and BACE1 (4X7I). Site-specific docking was conducted at the native ligand binding pocket, using memantine, rivastigamine, marplan, galantamine, and LY2886721 as respective controls. The results, detailed in Fig. 3.1 and Table 3.1, demonstrate that many WSbcompounds, notably Quercetin, Anahygrine, L-ascorbic acid, DL-tryptophan, and Withanolides, exhibited binding energies superior to their respective controls, indicating stronger and more stable ligand-protein complexes (lower binding energy signifies a more stabilized interaction). Furthermore, the docking analysis revealed that the favourable compounds were stabilized by the same key amino acid residues as their controls. Specifically, Quercetin, a known enhancer of neuronal longevity and neurogenesis, showed competitive binding. Anahygrine, an alkaloid unique to WS with previously reported multi-target inhibition (e.g., APP, EGFR, MAPK1, JUN), also demonstrated strong affinity. L-ascorbic acid, a potent antioxidant, and DL-tryptophan, a precursor to the neurotransmitter serotonin, presented significant binding. Lastly, Withanolides, recognized for their acetylcholinesterase inhibitor and NMDA antagonist properties relevant to neuroinflammation, also displayed promising docking scores. The free energies of protein-ligand complexes were computed using Prime's MM-GBSA, and the outcomes show the complexes' improved stability. The compounds will be more stable if the energies are more negative. Compared to controls, all of WS phytocompounds have higher negative free energy.

Table 3.1: Top Docking Hits: Top binding affinities of the primary phytochemical constituents of *Withania somnifera* with the target proteins.

Target Protein and Reference drug (score)	Rank	Ligand	Docking score
1PBQ NMDA receptor **Memantine (-3.41)**	**1**	**DL-Tryptophan**	**-9.53**
	2	Quercetin	-8.17
	3	Glutamate	-7.85
	4	DL-Aspartic acid	-7.77
	5	Nitrazepam	-7.57
4X7I BACE1 **LY2886721 (-9.35)**	**1**	**Quercetin**	**-8.28**
	2	Hydrocortisone	-6.78
	3	Withanolide N	-6.75
	4	Withanolide R	-6.60
	5	Withanolide J	-6.49
4EY6 Acetylcholinesterase **Galantamine (-8.01)**	**1**	**Anahygrine**	**-11.96**
	2	Cusoanahygrine	-11.60
	3	Quercetin	-11.43
	4	(-)-Anaferine	-11.12
	5	Nitrazepam	-9.88
2Z5X Monoamine oxidase A	**1**	**Quercetin**	**-10.01**
	2	L-Ascorbic acid	-9.65
	3	Resveratrol	-7.22

Table 3.1: Top Docking Hits: Top binding affinities of the primary phytochemical constituents of *Withania somnifera* with the target proteins.

Marplan (-6.95)	4	Scopoletin	-7.10
10PM Butyrylcholinesterase **LY2886721 (-1.97)**	**1**	**Quercetin**	**-10.34**
	2	Withanolide E	-7.41
	3	Cuscohygrine	-7.01
	4	Withanolide F	-6.92
	5	L-Arabinose	-6.61

Table 3.2 shows how some of the compounds from *W. somnifera* show better binding energies across all the target proteins

Table 3.2: Multi-Target Table: Top binding affinities of the top ligands across different proteins

Ligand | Proteins	1PBQ	4X7I	4EY6	2Z5X	10PM
Quercetin	-8.17	-8.28	-11.43	-10.01	-10.34
Anahygrine	-4.14	-5.39	**-11.96**	-	-4.74
Nitrazepam	-7.57	-5.38	-9.88	-	-5.75
Resveratrol	-5.05	-5.86	-	-7.22	-6.52
L-Ascorbic acid	-5.68	-	-9.68	-9.65	-5.85

a)

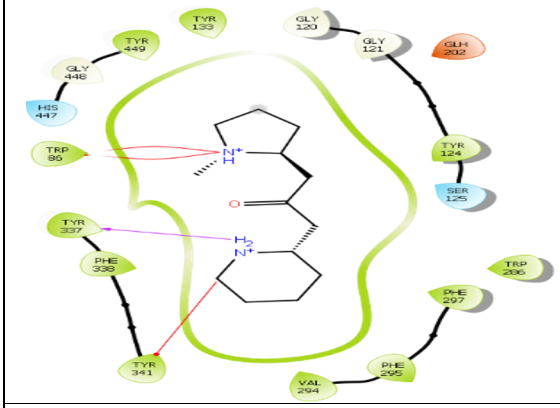

AChE: Anahygrine

b)

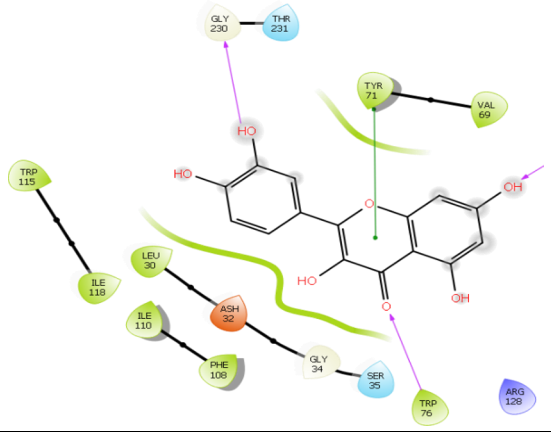

BACE1: Quercetin

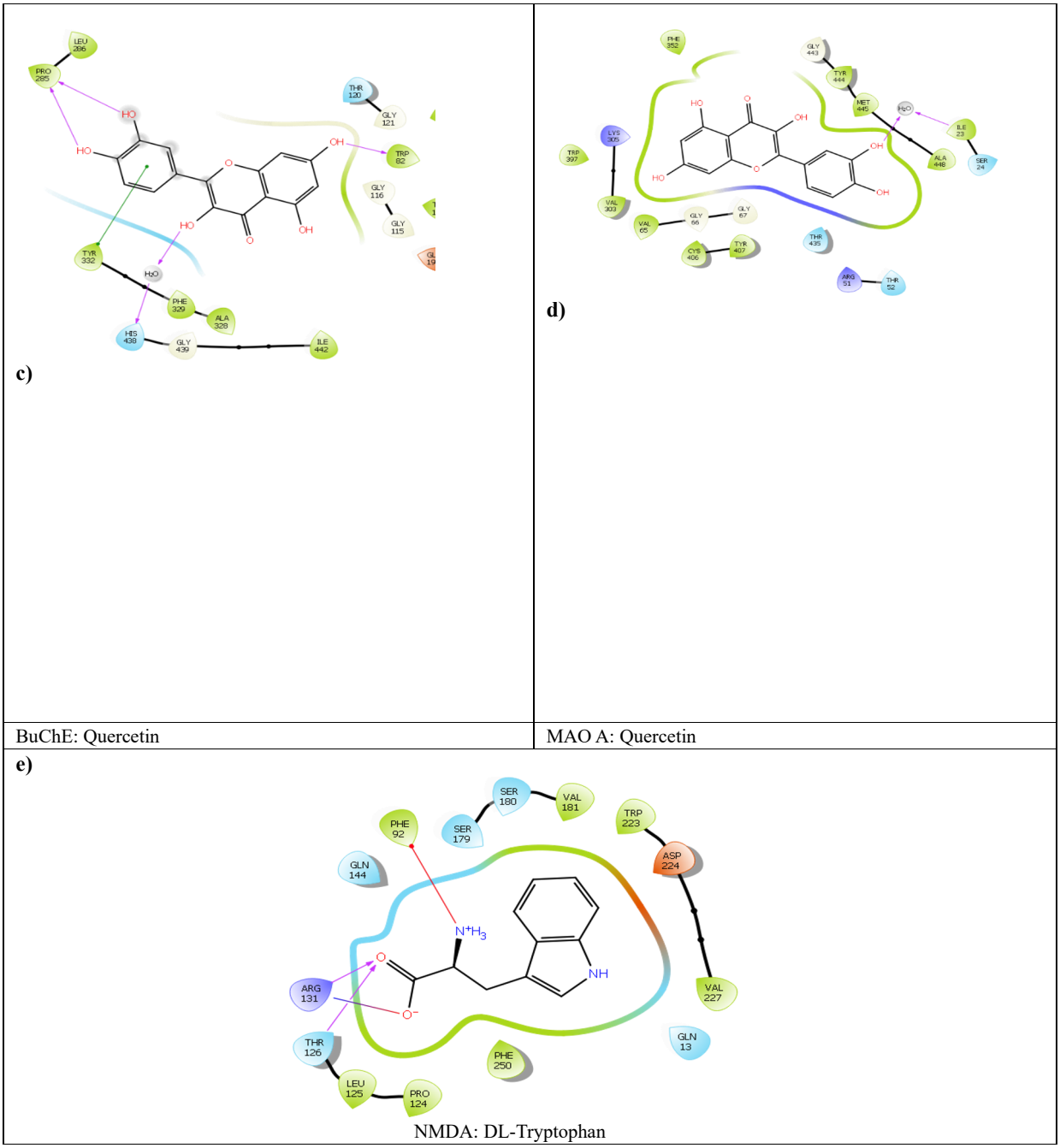

Figure 3.1 2D Ligand interaction diagram of top phytocompound of W. *somnifera* with target proteins. a) AChE: Anahygrine; b) BACE1: Quercetin; c) BuChE: Quercetin; d) MAO A: Quercetin; e) NMDA: DL-Tryptophan

3.2 Free Energy Calculations Using MM-GBSA

The free energies were calculated using the MM-GBSA of the Prime module in Schrodinger package. The more negative value represents the stability and binding of the complex. Table 3.3 shows the free energies of the binding complexes that have greater binding affinities than complex.

Table 3.3. Free energies of protein ligand complexes

4X7I (BACE1)	**ΔG (kcal/mol)**	**1PBQ (NMDA)**	**ΔG (kcal/mol)**	**10PM (BuChE)**	**ΔG (kcal/mol)**	**4EY6 (AChE)**	**ΔG (kcal/mol)**	**2Z5X (MAO-A)**	**ΔG (kcal/mol)**
LY2886721 (control)	-71.74	Memantine (control)	-41.52	Rivastigmine (control)	-21.23	Galantamine (control)	-59.49	Marplan (control)	-58.43
Quercetin	-41.58	DL-Tryptophan	-37.42	Quercetin	-38.28	Anahygrine	-54.83	Querceti n	-77.70
Hydrocortisone	-71.29	Quercetin	-62.74	Withanolide E	-62.07	Cuscohygrine	-58.58	LAscorbic acid	-43.79
Withanolide N	-80.16	Glutamate	-33.10	Cuscohygrine	-56.15	Nitrazepam	-44.18	Scopolet in	-49.39
Withanolide R	-69.53	DL-Aspartic acid	-28.08	Withanolide F	-53.84	L-Ascorbic acid	-31.53	-	-
Withanolide J	-76.24	Nitrazepam	-61.15	L-Arabinose	-26.77	-	-	-	-
24,25dihydrowithanolide D	-82.20	Withanolide F	-25.07	Resveratrol	-35.60	-	-	-	-
Withaferin A	-61.32	DL-Valine	-28.19	DL-Tryptophan	-26.81	-	-	-	-
Withanolide Q	-71.30	Creatine	-39.35	(-)-Anaferine	-57.08	-	-	-	-
-	-	L-Proline	-31.08	-	-	-	-	-	-

3.3. Quantitative Phytochemical Analysis of WS Extract

In order to characterize the extract to be used for the preparation of nano-emulsions, various qualitative and quantitative estimations were performed. The qualitative analysis of the procured extract of *W. somnifera* extract was done, wherein it was subjected for analyzing the presence of various phytocompounds: phenols, flavonoids, glycosides, alkaloids, saponins, triterpenoids and tannins. The presence of these phytocompounds was reported in the Indian herbal pharmacopeia and hence, it was tested in the extract to confirm the same. These listed compounds were found to be present in the extract as indicated in table by their specific color development during the respective assays performed. Results have shown that *W. somnifera* doesn't contain Saponins and Tannins. The quantitative analysis of the major group of phytochemicals, phenols and flavonoids in the extract: was performed, as they are reported to be present in higher quantity in the extract. Different assays, including biochemical assays, liquid chromatography–mass spectrometry (LC–MS) were performed to estimate their amount in the extract. The results obtained from all these analyses are discussed below.

A) Liquid Chromatography Mass Spectrometry Analysis of WS

The standard extract WS was further verified for its major active principles, which are: Quercetin, Nitrazepam, and Lascorbic acid. The standard graphs with the pure compounds of the listed phytocompound were plotted to estimate the presence of the same compounds in the extract.

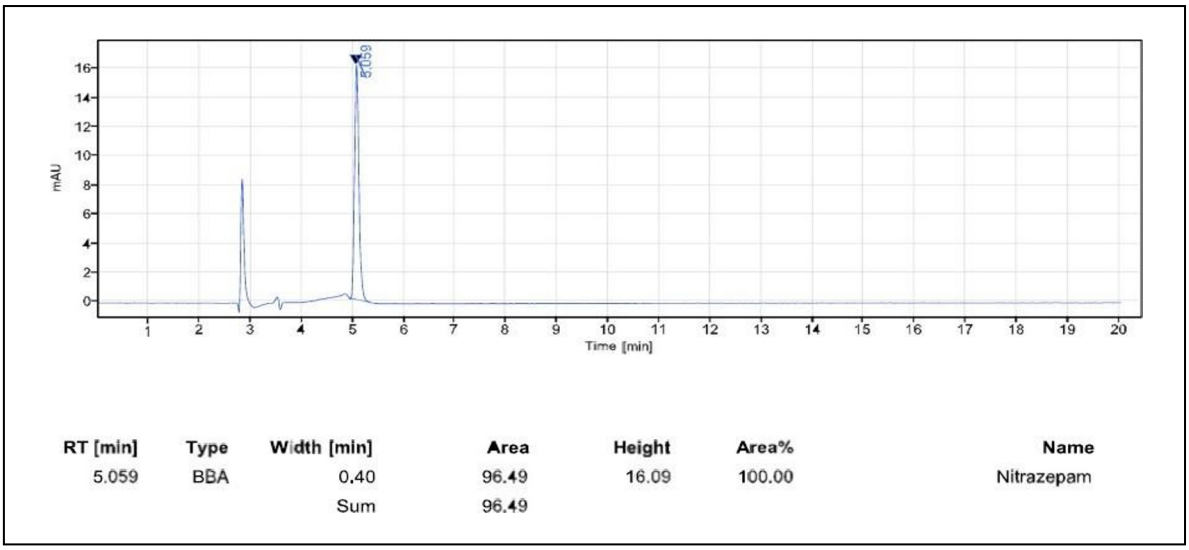

RT [min]	Type	Width [min]	Area	Height	Area%	Name
5.059	BBA	0.40	96.49	16.09	100.00	Nitrazepam
		Sum	96.49			

Figure 3.2 (a): Standard chromatogram of Nitrazepam by LC – MS estimation.

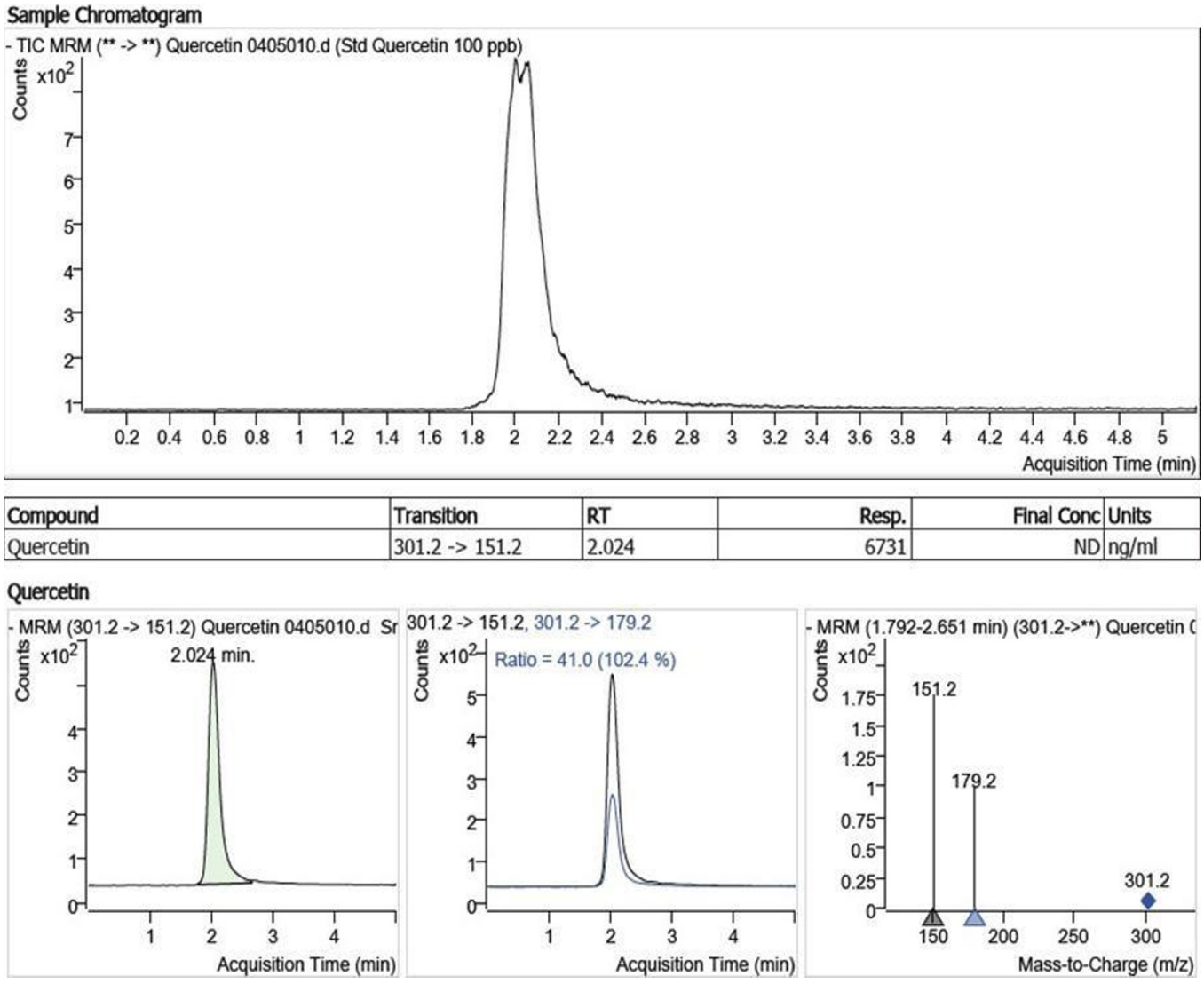

Compound	Transition	RT	Resp.	Final Conc	Units
Quercetin	301.2 -> 151.2	2.024	6731	ND	ng/ml

Figure 3.2 (b): Standard chromatogram of Quercetin by LC – MS estimation

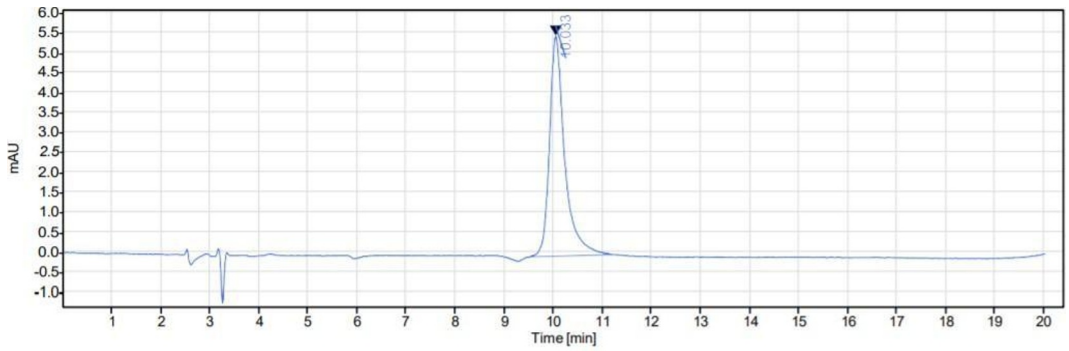

RT [min]	Type	Width [min]	Area	Height	Area%	Name
10.033	BB	1.69	117.90	5.47	100.00	Vitamin C
		Sum	117.90			

Figure 3.2. (c): Standard chromatogram of L-Ascorbic acid by LC – MS estimation **3.4**

Preparation of WSNE

a) Titration Study

Following the solubility results, the WS extract formulation was examined using the aqueous phase titration method, in which the extract was combined with the excipients (ethanol, triacetin, and almond oil) that had the highest solubility for the extract. These three combinations of surfactant and co-surfactants with distinct titration ratios were chosen for additional analysis out of the 112 combinations that were tested (Table 3.4). Here, a combination of surfactants and co-surfactants is referred to as "Smix." Additionally, the extracts with a Smix ratio of 2:1 demonstrated the highest clear titration combinations out of all the combinations (almond oil, triacetin, and ethanol) with a Smix ratio of 7:3, therefore they were taken into consideration for additional testing.

Table 3.4. (a) Excipient combinations with their Smix ratios and attained clear titration zones in *W. somnifera*

S.No.	**Combination**	**Smix Ratios**	**Clear Titration Ratios**
1	Almond oil + Triacetin (Glycerol triacetate) + Ethanol [WSNE - 1]	1:0	1:9. 2:8. 4:6, 5:5, 6:4, 7:3, 8:2, 9:1, 1:2, 1:3, 1:3.5, 1:5, 1:6, 1:7, 1:8
2	Almond oil + Triacetin (Glycerol triacetate) + Ethanol [WSNE - 2]	1:1	2:8, 3:7, 4:6, 5:5, 6:4, 7:3, 8:2, 9:1, 1:2, 1:3, 1:3.5, 1:5, 1:6, 1:7, 1:8
3	Almond oil + Triacetin (Glycerol triacetate) + Ethanol [WSNE - 3]	2:1	1:9, 2:8, 3:7, 4:6, 5:5, 6:4, 7:3, 8:2, 9:1, 1:2, 1:3, 1:3.5, 1:5, 1:6, 1:7, 1:8
4	Almond oil + Triacetin (Glycerol triacetate) + Ethanol [WSNE - 4]	3:1	1:9, 2:8, 3:7, 4:6, 5:5, 6:4, 7:3, 8:2, 9:1, 1:2, 1:3, 1:3.5, 1:5, 1:6, 1:7, 1:8
5	Almond oil + Triacetin (Glycerol triacetate) + Ethanol [WSNE - 5]	4:1	1:9, 2:8, 3:7, 4:6, 1:2, 1:3, 1:3.5, 1:5, 1:6, 1:7, 1:8

6	Almond oil + Triacetin (Glycerol triacetate) + Ethanol [WSNE - 6]	5:1	1:9, 2:8, 1:2, 1:3, 1:3.5, 1:5, 1:6, 1:7, 1:8
7	Almond oil + Triacetin (Glycerol triacetate) + Ethanol [WSNE - 7]	6:1	1:9, 2:8, 1:2, 1:3, 1:3.5, 1:5, 1:6, 1:7, 1:8

b) Preparation of Pseudoternary Diagram

By illustrating the connection between a mixture's phase behavior and composition, a pseudo-ternary phase diagram plot was developed to indicate the existence range of nano-emulsions. For every Smix ratio, separate pseudo-ternary phase diagrams were made in order to determine the o/w nano-emulsion regions.. The isotropic zone shifted towards Smix when the surfactant ratio was raised. The Smix form of these two components must have higher solubility and stability. The clear and homogeneous solutions are indicated by the area of solubilization in phase diagrams [46].

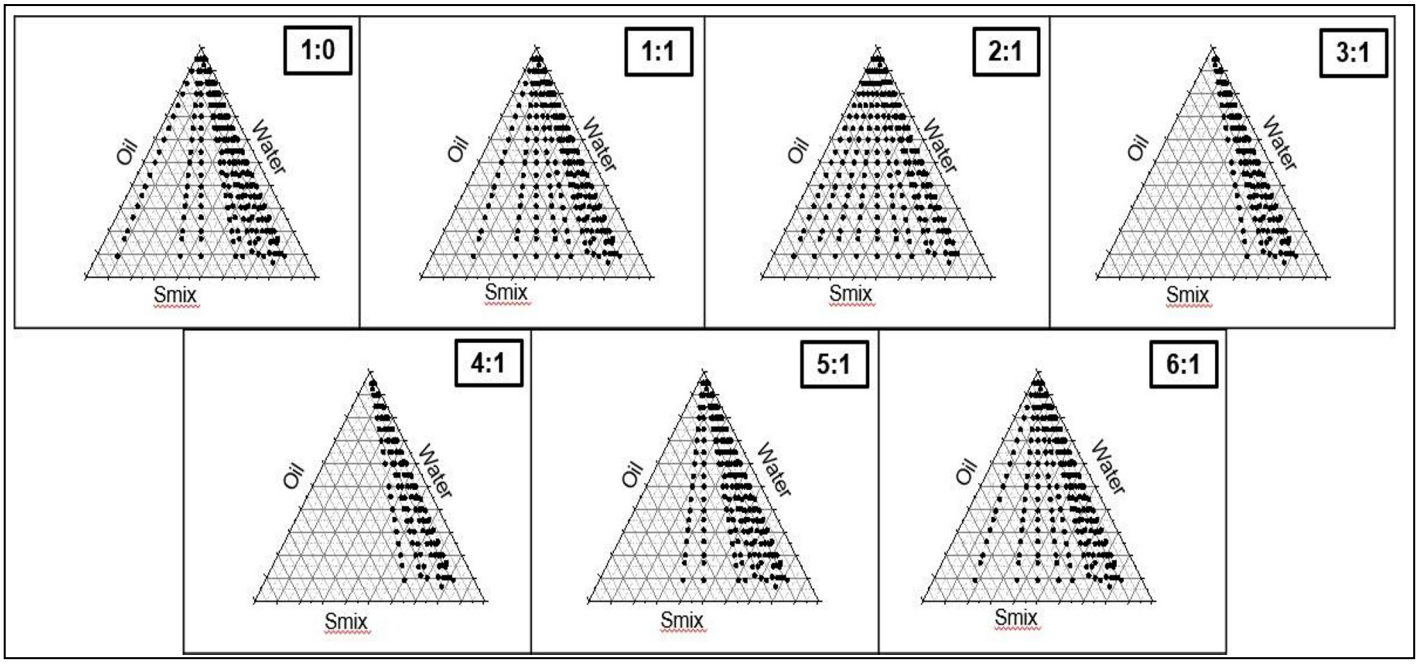

Figure 3.3. Showing pseudo ternary phase diagram indicating o/w nano-emulsions using Almond oil (Oil), Triacetin (Surfactant) and ethanol (Co surfactant) with all Smix ratio of *W. somnifera*

3.5. Characterization of WSNE

The optimized formulation was characterized for its thermodynamic stability by evaluating the parameters mentioned above in Table 3.4.

3.5.1. Thermodynamic stability studies

The extract loaded combination ratios of the excipients were then tested further for their thermodynamic stability by subjecting them in various physical conditions like temperature variations (45, 4, (-) 4 and 37°C), speed variation (centrifugation at 1250Xg) and aqueous dispersibility. There were five samples that cleared the test with the highest thermodynamic stability and out of them three best formulations with “Grade A” were accepted and analyzed further. 1:0, 1:1, 2:1, and 3:1 Smix Ratios were accepted on the basis of all four cycles, ability to resist heating cooling cycle, freezethaw cycle, centrifugation and dispersibility test of *W. somnifera* nanoemulsions.

3.5.2. Particle size analysis (psa) and polydispersity (pdi) analysis

After determining the thermodynamic stability of all the nanoemulsions generated, specific formulations from *W. somnifera* were chosen for further analysis. The droplet size of all nano-emulsions, with droplet sizes ranging from nano to micro, using a zeta particle size analyzer. For further investigation, the polydispersity index and particle size were chosen. The Polydispersity Index, which ranges from 0 to 1, indicates the width of the particle size distribution, reflecting the kind of

dispersion. PDI values less than 0.5 are considered to have the best dispersion quality and demonstrate a limited size distribution [48].

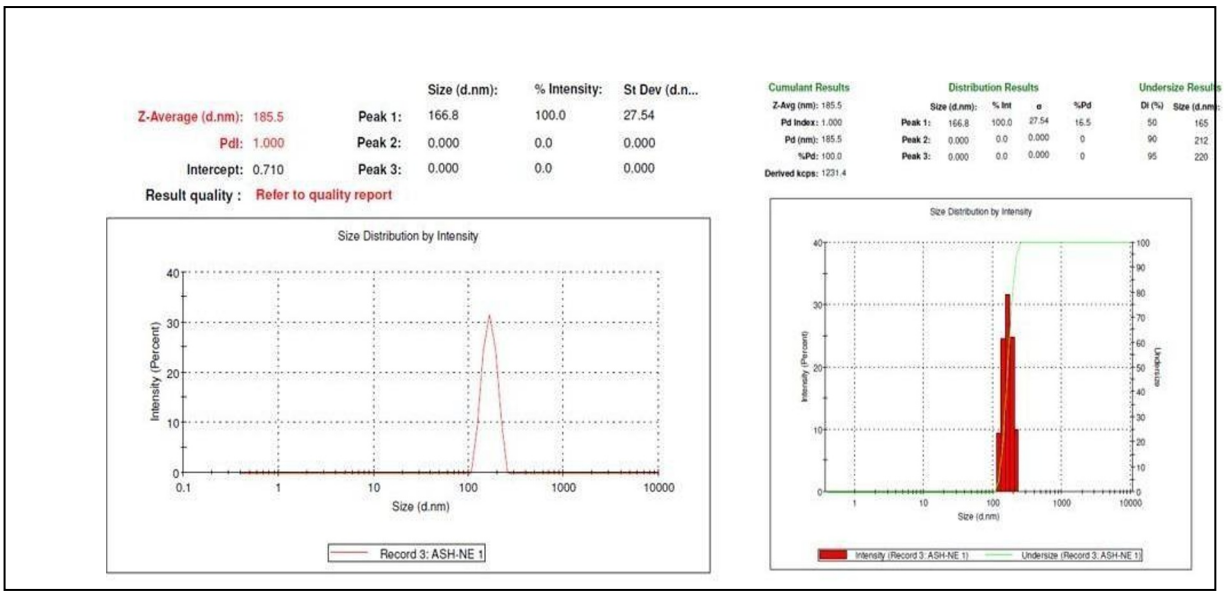

Figure 3.4 Summarization of Particle size and Polydispersity Index of the optimized nano-emulsions of *W. somnifera*

Experiments with the other combination of excipients revealed a smaller size range when compared to the size of nanoemulsions reported in the literature. In the current work, however, the spherical radius (nm) is significantly larger, which could be related to the fact that both extracts contain a complex combination rather than a pure chemical. The PDI value of the optimized extract nano-emulsions is 1 and 0.540, indicating a moderately homogeneous distribution of nano-emulsions.

3.5.3. Zeta potential (zp) analysis

The existence of charge (positive or negative) on the particle's surface determines its electric potential and polarity, which are reflected in the formulation's zeta potential [49]. Withania somnifera's optimized formulation had a zeta potential of (-) 33.3 mV, whereas Bacopa monnieri's optimized formulation had a zeta potential of (-) 28.4 mV. This suggests that the surfactant triacetin has both ionic and non-ionic phase nature, which lowers the zeta potential charges on the surface of micelles formed, resulting in the prevalence of repulsive forces and preventing flocculation [49].

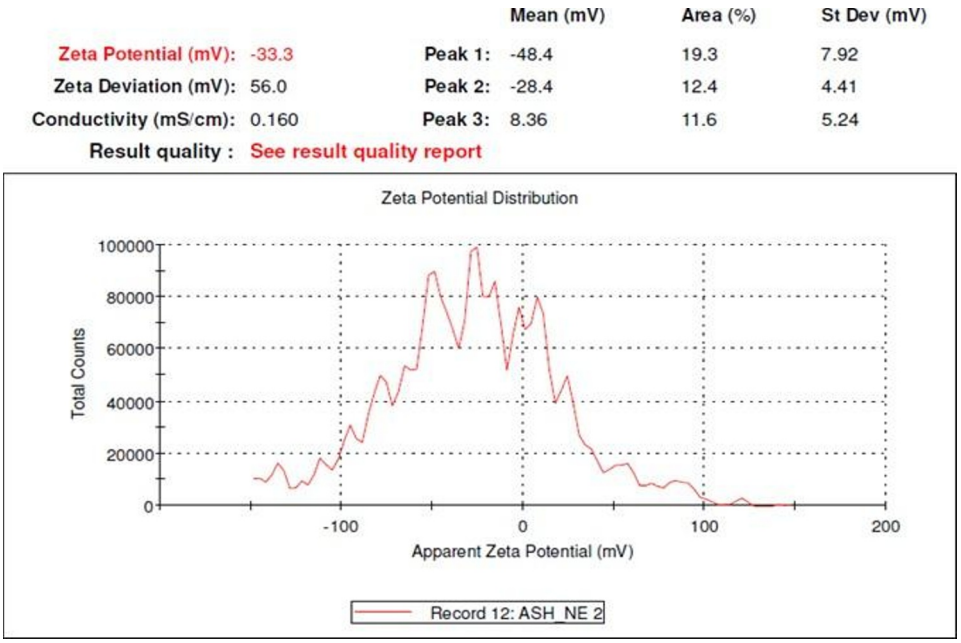

Figure 3.5. Zeta Potential of the optimized nano-emulsions of *W. somnifera*

3.5.4. Transmission electron microscopy (TEM) analysis

Various scientists have utilized TEM to analyze and validate particle size and shape. Figures 3.6 (a) and (b) display TEM micrographs of the particles of the enhanced formulation of Withania somnifera. Particles in the spherical nanometric size range (150 nm to 300 nm) were found to be finely distributed. The globule diameters of *Withania somnifera* nano-emulsions derived from TEM images are therefore in agreement with an earlier particle size analyzer investigation.

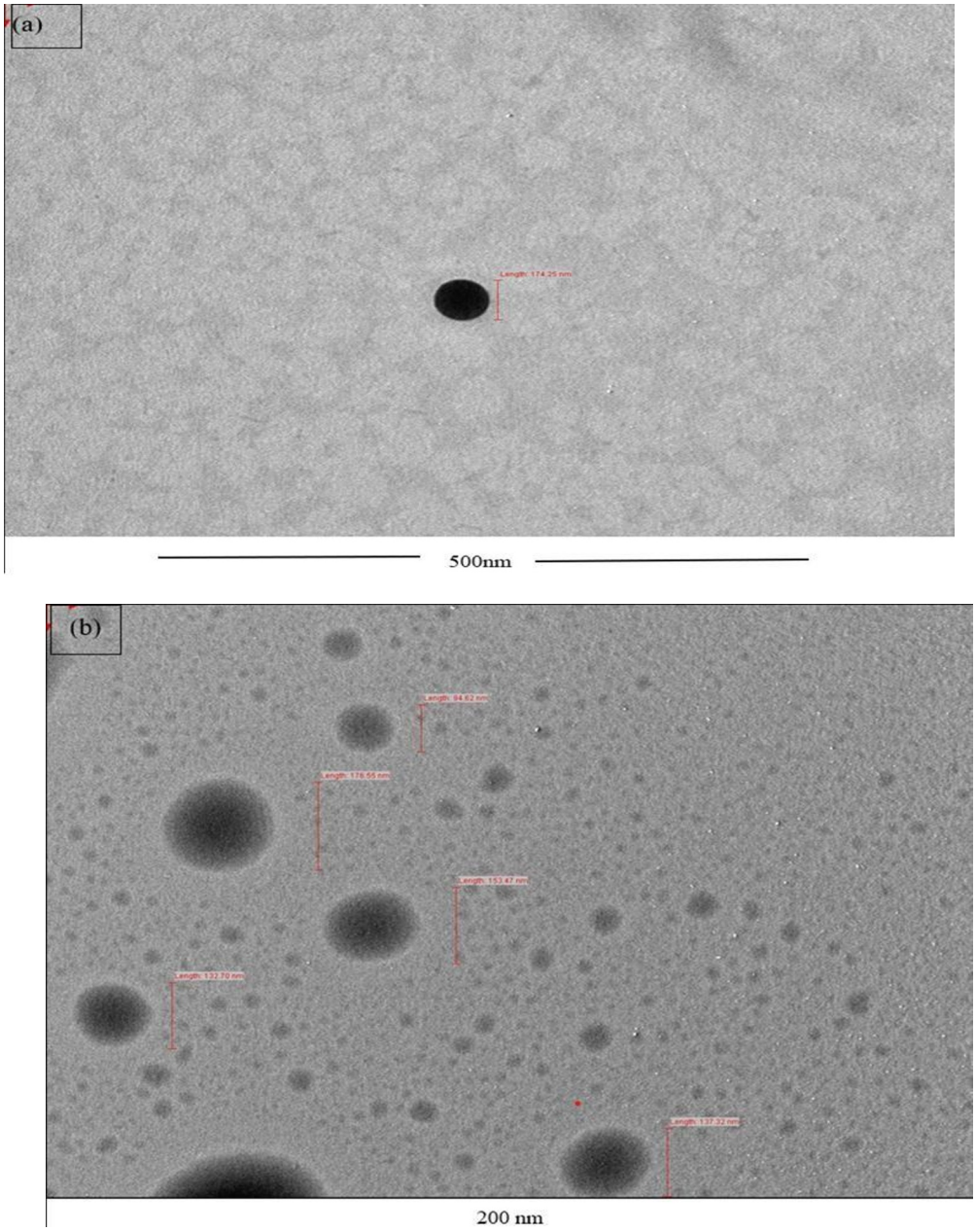

Figure 3.6. (a) and (b) TEM image of the optimized *W. somnifera* extract loaded nano-emulsions at 40,000x and 80,000x magnifications (scale bar showing 200 and 500 nm range)

3.5.5. Measurement of rheological and other parameters

3.5.5.1. Viscosity

The viscosities of nano-emulsions are influenced by the oil's molecular volume and effective carbon number. Because almond oil contains a saturated long chain with efficient carbon numbers, making it more flowable, it was chosen for the oil phase of this study [43]. Triacetin is combined with ethanol as a co-surfactant in this work because alcohols are thought to join the micelle interface by positioning themselves among surfactant heads.

3.5.5.2. Conductivity

The specific conductivity of nano-emulsions was found to be 61.3 and 86.8 mS/m.

3.5.5.3. pH

The pH of *W. somnifera* is 4.20, which is a little less than the optimum pH that needs to be required in the brain region (pH- 7.2)

Table 3.5. Summary of the optimized nano-emulsions' rheological characteristics.

Sample	pH	Conductivity (mS/cm)	Viscosity (cP)
ASH Bare nano- emulsion	3.88 ± 0.27	66.1 ± 0.6	32.3 ± 0.2
ASH-ALGA	4.20 ± 0.5	61.3 ± 0.5	± 0.6

3.5.5.4. Investigation of internalization of extract: FT-IR analysis

FTIR spectroscopy was performed for extract, optimized bare nano-emulsions of selected concentration and, optimized nano-emulsions with *Withania somnifera* respectively. The samples were scanned for absorbance over range from 4,000 to 400 wave numbers (cm–1) [42]. The significant peaks of flavone group (1028 - 1649 cm–1) were observed in scan of the extract. These peaks were not reflected in the scan of extract loaded nano emulsion indicating that the functional groups for extract have been masked by the excipients and hence, the signature peaks of the extract are not visible in the graph. Therefore, it can be concluded from the observations that there was no flavonone glycosides were present on the outer surface of the nano-emulsion.

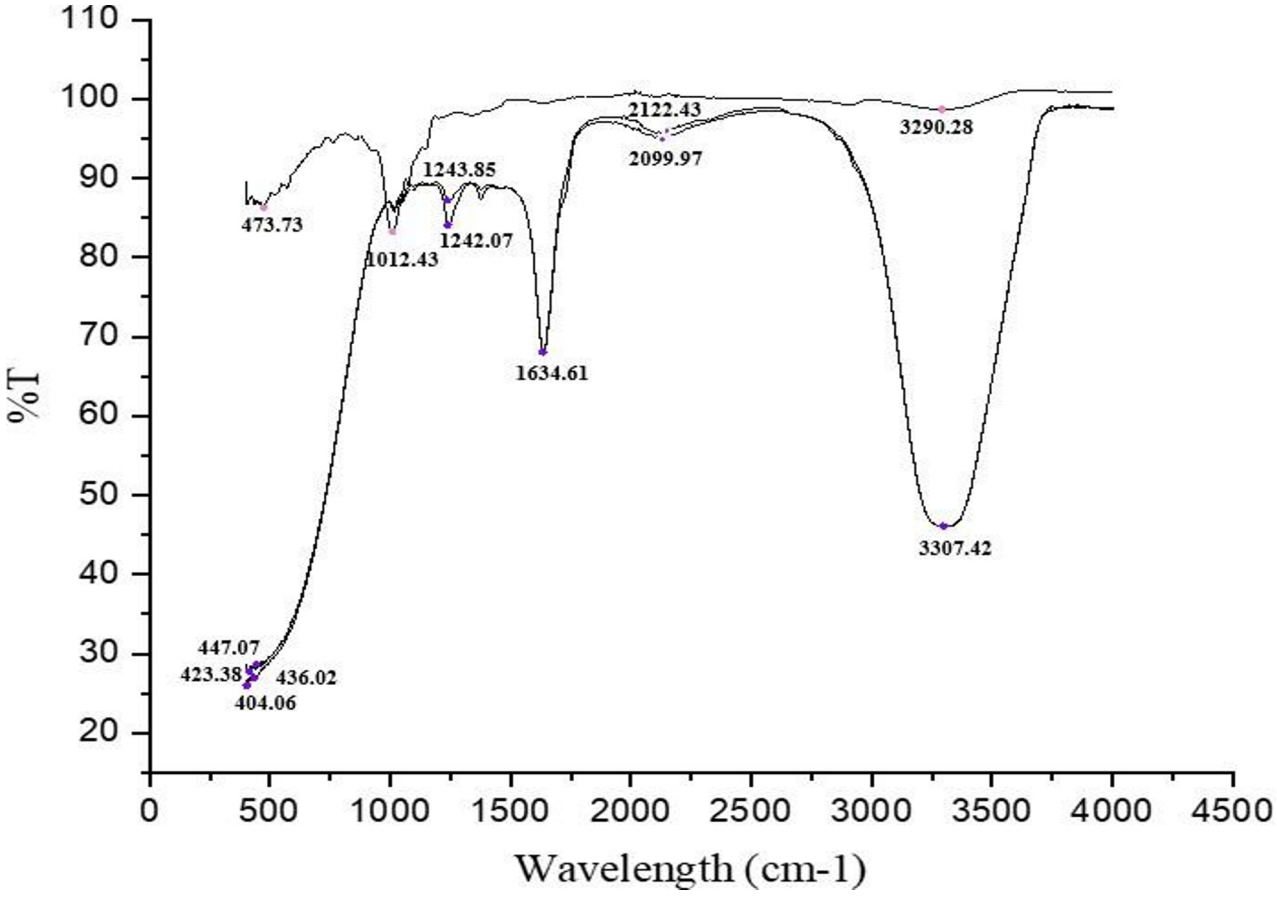

Figure 3.6. FT – IR analysis of the plain *W. somnifera* extract, optimized *W. somnifera* loaded nano-emulsions

Discussion

The study initiated with *in silico* studies that were designed to target five targets of AD, and conducted to check the efficacy of selected phytocompounds against them. From the results, it was very clear that the phytocompounds from *Withania somnifera* have better efficacy than the standard control drug. Even the

amino acids involved in the interaction also shows resemblances with control drug. Taking the points from *in silico* studies, these plants were further analysed and their oil-in-water nanoemulsions were made. After various preliminary studies of *W. somnifera* loaded oil in water (o/w) nano-emulsions system was prepared with a 20mg/ml of NE excipients (20mg *W. somnifera* eq./ml, respectively) and depending on the solubility index of extract in various excipients, Almond oil, Triacetin and Ethanol were selected for oil, surfactant and co surfactant phases; respectively along with distil water as an aqueous phase. Thereafter, ternary phase diagrams were plotted as per the excipient ratios used and clear zones obtained, this type of combination and its ratio optimization was also supported by Trotta et al., 1995 [47] with same Smix combination ratios. Similar NE system was developed by various other researchers also like – Shafiq et al, 2007 [48], where he developed ramipril nano-emulsions.

The formulation with maximum Oil:Smix ratio, clear zones were then opted as the optimized formulation (Smix Ratio of 2:1). The *Withania somnifera* loaded nano-emulison exhibited the particle size range of 188nm (DLS method) with Polydispersibility index (PDI) score ranging from 1 and zeta potential from -33.3 mV. As represented in table and out of the listed formulations, for the extract, 2:1 was selected as an optimized formulation for further experiments as it reflected the narrow size distribution (good PDI) and size range of 180 - 220 nm. Though the size range of NE droplets with same excipients and various other therapeutic compounds was found to be on slightly higher side in DLS results still being in the nanometric size range, the probability of its enhanced therapeutic efficiency was higher therefore, the same formulation sample was analyzed for TEM, where the micrographs of optimized formulation showed the NE droplets in nano metric size range (160- 330 nm), finely distributed and in spherical shape as represented. The same excipient components (Almond oil, triacetin and ethanol) with other pure compounds like acyclovir and diclofenac showed the size range below 50 nm, however our formulation (ITE A1) showed higher, we suggest that due to complex phytocompound combination present in the extract, higher particle size was obtained as similar explanation was provided by Pessoa et al, 2015 [49], where the group showed that the babassu (Orbignya/ Attalea) extract derived oil, which a wide variety of fatty acids and other phytocompounds when formulated for oil in water type nano-emulsions system, also showed the size above 250nm (277.40 nm) indicating that the complex extract mixture loaded nano-emulsions system tend to reflect the size range above 200 nm.

Simultaneously, the rheological parameters of the optimized formulations were evaluated and were found to be in the desirable ranges 34.3 and 41.1 cP .Similar to aqueous conductivity, the specific conductivity of nanoemulsions was determined to be 61.7 and 83.8 mS/m. The pH must be close to 6.7 because the exterior phase is watery. Additionally, Xu et al. [50] made similar observations, discussing how pH (4.5–6.8) and viscosity (30– 45 cP in the case of o/w nano-emulsions) parameters are crucial for the effective delivery of the therapeutic compound, particularly when it must be administered intranasally. FTIR analysis confirmed successful encapsulation of the extract within the nanoemulsion system. The masking of characteristic functional group peaks of the extract in the formulation spectrum suggested entrapment within the excipient matrix without evidence of significant chemical interaction or complex formation. Overall, the findings indicate that optimized nanoemulsion system provides a stable and promising delivery mechanism, however, further validation through detailed in vitro and in vivo investigations is necessary to establish its therapeutic efficacy and translational potential.

CONCLUSION

Withania somnifera extract-loaded nano-emulsions are found to be stable under various thermodynamic and physiochemical analysis. *W. somnifera* extract loaded nano-emulsions having particle size in micro - nano metric range were successfully developed and characterized.

According to the improved formulation's characterisation, its size range is 180-260nm, and TEM confirmation shows that its zeta potential is between -28.8 and -33.3 Mv. To sum up, our study shows that the created formulation may have therapeutic benefits for reducing the degenerative state of AD and might be pursued as a viable option for clinical studies to assess its effectiveness in people.

References

[1] T. Wyss-Coray, "Ageing, neurodegeneration and brain rejuvenation," (in eng), Nature, vol. 539, no. 7628, pp. 180–186, 2016.

[2] WHO, "Dementia," 2021.

[3] R. C. Petersen et al., "Alzheimer's disease," Seminars in Neurology, vol. 37, no. 3, pp. 227–237, 2017.

[4] D. S. Knopman et al., "Alzheimer disease," Nature Reviews Disease Primers, vol. 7, no. 1, p. 33, 2021.

[5] W. M. van der Flier and P. Scheltens, "Epidemiology and risk factors of dementia," Journal of Neurology, Neurosurgery & Psychiatry, vol. 76, suppl. 5, pp. v2–v7, 2005.

[6] B. N. Dugger and D. W. Dickson, "Pathology of Neurodegenerative Diseases," Cold Spring Harbor Perspectives in Biology, vol. 9, no. 7, p. a028035, 2017.

[7] A. V. Terry Jr. and J. J. Buccafusco, "The cholinergic hypothesis of age and Alzheimer's disease-related cognitive deficits: recent challenges and their implications for novel drug development," (in eng), Journal of Pharmacology and Experimental Therapeutics, vol. 306, no. 3, pp. 821–827, 2003.

[8] A. D. Gitler, P. Dhillon, and J. Shorter, "Neurodegenerative disease: models, mechanisms, and a new hope," (in eng), Disease models & mechanisms, vol. 10, no. 5, pp. 499–502, 2017.

[9] L. Zhao, J. Li, H. Zhao, and T. Ye, "Mechanisms and interventions of oxidative stress-induced neurodegeneration," Redox Biology, vol. 64, p. 102778, 2023.

[10] J. Liu, L. Chang, Y. Song, H. Li, and Y. Wu, "The Role of NMDA Receptors in Alzheimer's Disease," (in English), Frontiers in Neuroscience, vol. 13, p. 43, 2019.

[11] R. Venkatesan, E. Ji, and S. Y. Kim, "Phytochemicals That Regulate Neurodegenerative Disease by Targeting Neurotrophins: A Comprehensive Review," BioMed Research International, vol. 2015, p. 814068, 2015.

[12] N. J. Abbott, A. A. K. Patabendige, D. E. M. Dolman, S. R. Yusof, and D. J. Begley, "Structure and function of the blood-brain barrier," Neurobiology of Disease, vol. 37, no. 1, pp. 13–25, 2010.

[13] J. Kreuter, "Nanoparticulate systems for brain delivery of drugs," Advanced Drug Delivery Reviews, vol. 64, pp. 213–222, 2012.

[14] A. Teleanu, C. Niculescu, R. Teleanu, and D. M. Mitrea, "Blood-brain barrier disruption in neurological disease and therapy," (in eng), International Journal of Molecular Sciences, vol. 23, no. 7, p. 3782, 2022.

[15] M. Kolarova, F. García-Sierra, A. Bartos, J. Ricny, and D. Ripova, "Structure and pathology of tau protein in Alzheimer disease," (in eng), Int J Alzheimers Dis, vol. 2012, p. 731526, 2012.

[16] G. C. Bhatt, S. Bhattacharya, and T. Mehta, "Prevalence and etiology of dementia: a systematic review and meta-analysis," Neurological Sciences, vol. 44, no. 4, pp. 1227–1239, 2023.

[17] M. Cummings, J. Zhou, G. Lee, D. Zhong, and T. Fonseca, "Lecanemab: appropriate use recommendations," Journal of Prevention of Alzheimer's Disease, vol. 10, no. 3, pp. 362–377, 2023.

[18] M. Esiri et al., "Cerebral amyloid angiopathy, subcortical white matter disease and dementia: literature review and study in OPTIMA," (in eng), Brain pathology (Zurich, Switzerland), vol. 25, no. 1, pp. 51–62, 2015.

[19] J. Pradeepkiran and P. H. Reddy, "Defective mitophagy in Alzheimer's disease," (in eng), Ageing Research Reviews, vol. 64, p. 101191, 2020.

[20] H. Hampel et al., "The cholinergic system in the pathophysiology and treatment of Alzheimer's disease," Brain, vol. 141, no. 7, pp. 1917–1933, 2018.

[21] H. Hampel et al., "Revisiting the Cholinergic Hypothesis in Alzheimer's Disease: Emerging Evidence from Translational and Clinical Research," (in eng), J Prev Alzheimers Dis, vol. 6, no. 1, pp. 2–15, 2019.

[22] J. Cao, X. Hou, J. Ping, and H. Cai, "Advances in developing novel therapeutic strategies for Alzheimer's disease," Molecular Neurodegeneration, vol. 13, no. 1, p. 64, 2018.

[23] H. Hampel et al., "The Amyloid-β Pathway in Alzheimer's Disease," Molecular Psychiatry, vol. 26, no. 10, pp. 5481–5503, 2021.

[24] Z. Cai, "Monoamine oxidase inhibitors: promising therapeutic agents for Alzheimer's disease (Review)," (in eng), Mol Med Rep, vol. 9, no. 5, pp. 1533–41, May 2014.

[25] W. L. Jorgensen, D. S. Maxwell, and J. Tirado-Rives, "Development and Testing of the OPLS All-Atom Force Field on Conformational Energetics and Properties of Organic Liquids," Journal of the American Chemical Society, vol. 118, no. 45, pp. 11225–11236, 1996.

[26] D. Shivakumar et al., "Prediction of Absolute Solvation Free Energies using Molecular Dynamics Free Energy Perturbation and the OPLS Force Field," Journal of Chemical Theory and Computation, vol. 6, no. 5, pp. 1509–1519, 2010.

[27] A. G. Atanasov et al., "Natural products in drug discovery: advances and opportunities," Nature Reviews Drug Discovery, vol. 20, no. 3, pp. 200–216, 2021.

[28] J. C. Shelley et al., "Epik: a software program for p^{a}a prediction and protonation state generation/enumeration," Journal of Computer-Aided Molecular Design, vol. 21, no. 12, pp. 681–691, 2007.

[29] R. A. Friesner et al., "Glide: A New Approach for Rapid, Accurate Docking and Scoring. 1. Method and Assessment of Docking Accuracy," Journal of Medicinal Chemistry, vol. 47, no. 7, pp. 1739–1749, 2004.

[30] S. Forli et al., "Computational protein–ligand docking and virtual drug screening with the AutoDock suite," Nature Protocols, vol. 11, no. 5, pp. 905–919, 2016.

[31] P. D. Lyne, M. L. Lamb, and J. C. Saxton, "Accurate prediction of the relative potencies of members of a series of kinase inhibitors using molecular docking and MM-GBSA scoring," Journal of Medicinal Chemistry, vol. 49, no. 16, pp. 4805–4808, 2006.

[32] R. A. Friesner et al., "Extra Precision Glide: Docking and Scoring Incorporating a Model of Hydrophobic Enclosure for Protein–Ligand Complexes," Journal of Medicinal Chemistry, vol. 49, no. 21, pp. 6177–6196, 2006.

[33] T. A. Halgren et al., "Glide: a new approach for rapid, accurate docking and scoring. 2. Enrichment factors in database screening," (in eng), J Med Chem, vol. 47, no. 7, pp. 1750–1759, Mar 25 2004.

[34] R. Abel, L. Wang, E. D. Harder, B. J. Berne, and R. A. Friesner, "Advancing Drug Discovery through Enhanced Free Energy Calculations," Accounts of Chemical Research, vol. 50, no. 7, pp. 1625–1632, 2017.

[35] A. Daina, O. Michielin, and V. Zoete, "SwissADME: a free web tool to evaluate pharmacokinetics, drug-likeness and medicinal chemistry friendliness of small molecules," Scientific Reports, vol. 7, no. 1, p. 42717, 2017.

[36] C. A. Lipinski, "Rule of five in 2015 and beyond: target and ligand structural limitations, ligand chemistry structure and drug discovery project decisions," Advanced Drug Delivery Reviews, vol. 101, pp. 34–41, 2016.

[37] P. Banerjee, A. O. Eckert, A. K. Schrey, and R. Preissner, "ProTox-II: a webserver for the prediction of toxicity of chemicals," (in eng), Nucleic acids research, vol. 46, no. W1, pp. W257–W263, 2018.

[38] J. Redfern, M. Kinninmonth, D. Burdass, and J. Verran, "Using soxhlet ethanol extraction to produce and test plant material (essential oils) for their antimicrobial properties," (in eng), Journal of microbiology & biology education, vol. 15, no. 1, pp. 45–46, 2014.

[39] J. M. Dinore and M. Farooqui, "GC-MS and LC-MS: an integrated approach towards the phytochemical evaluation of methanolic extract of Pigeon Pea [Cajanus cajan (L.) Millsp] leaves," (in eng), Natural Product Research, vol. 36, no. 8, pp. 2177–2181, 2022.

[40] M. Trivedi et al., "Liquid Chromatography – Mass Spectrometry (LC-MS) Analysis of Withania somnifera (Ashwagandha) Root Extract Treated with the Energy of Consciousness," American Journal of Life Sciences, vol. 5, no. 1, pp. 21–30, 2017.

[41] M. Gupta, S. Thakur, A. Sharma, and S. Gupta, "Qualitative and Quantitative Analysis of Phytochemicals and Pharmacological Value of Some Dye Yielding Medicinal Plants," Oriental Journal of Chemistry, vol. 29, pp. 475–481, 2013.

[42] M. Mecozzi, M. Pietroletti, and M. Montalto, "Application of FTIR spectroscopy in environmental and materials science," Spectrochimica Acta Part A, vol. 281, p. 121571, 2022.

[43] M. Pal, J. Khushbu, S. Bhatt, and R. Vyas, "Rheological characterisation of nanoemulsions: influence of oil type and surfactant composition," Colloids and Surfaces A, vol. 648, p. 129290, 2022.

[44] E. Ashari, "Development of a kojic monooleate-enriched oil-in-water nanoemulsion as a potential carrier for hyperpigmentation treatment," International Journal of Nanomedicine, vol. 2018, pp. 6465–6479, 2018.

[45] M. S. Jangdey, A. Gupta, and S. Saraf, "Fabrication, in-vitro characterization, and enhanced in-vivo evaluation of carbopol-based nanoemulsion gel of apigenin for UV-induced skin carcinoma," (in eng), Drug delivery, vol. 24, no. 1, pp. 1026–1036, 2017.

[46] N. Sharma, S. Mishra, S. Sharma, R. Deshpande, and R. Sharma, "Preparation and Optimization of Nanoemulsions for targeting Drug Delivery," International Journal of Drug Development and Research, vol. 5, pp. 37–48, 2013.

[47] M. Trotta, E. Ugazio, and M. R. Gasco, "Pseudo-ternary phase diagrams of lecithin-based microemulsions: influence of monoalkylphosphates," (in eng), Journal of Pharmacy and Pharmacology, vol. 47, no. 6, pp. 451–454, 1995.

[48] S. Shafiq et al., "Development and bioavailability assessment of ramipril nanoemulsion formulation," (in eng), European Journal of Pharmaceutics and Biopharmaceutics, vol. 66, no. 2, pp. 227–243, 2007.

[49] R. S. Pessoa et al., "Microemulsion of babassu oil as a natural product to improve human immune system function," (in eng), Drug Design, Development and Therapy, vol. 9, pp. 21–31, 2015.

[50] J. Xu, J. Tao, and J. Wang, "Design and Application in Delivery System of Intranasal Antidepressants," (in English), Frontiers in Bioengineering and Biotechnology, Review vol. 8, 2020-December-21 2020.